Targeting Strategies for Cancer Radiotherapy[1]

Donald J. Buchsbaum,[2] Buck E. Rogers, M. B. Khazaeli, Matthew S. Mayo, Diane E. Milenic, S. V. S. Kashmiri, Carolyn J. Anderson, Lara L. Chappell, Martin W. Brechbiel, and David T. Curiel

Departments of Radiation Oncology [D. J. B., B. E. R.], Medicine [M. B. K., D. T. C.], and Gene Therapy Center [D. T. C.], University of Alabama at Birmingham, Birmingham, Alabama 35233; Department of Preventive Medicine [M. S. M.], University of Kansas Medical Center, Kansas City, Kansas 66160; Laboratory of Tumor Immunology and Biology [D. E. M., S. V. S. K.] and Radioimmune and Inorganic Chemistry Section [L. L. C., M. W. B.], National Cancer Institute, NIH, Bethesda, Maryland 20892; and Mallinckrodt Institute of Radiology [C. J. A.], Washington University School of Medicine, St. Louis, Missouri 63110

Abstract

Novel strategies to increase the therapeutic ratio in clinical radioimmunotherapy studies are needed. Limitations to radioimmunotherapy include bone marrow suppression due to the long circulating half-life of radiolabeled monoclonal antibodies (mAbs) and heterogeneous tumor penetration of the high-molecular-weight mAb. An approach to overcome these problems is the use of genetically engineered mAbs. The engineered mAb discussed in this paper contains a deletion in the constant region of the mAb that increases its tumor penetration and blood clearance compared with the intact mAb. Radiolabeling of this mAb should lead to a similar radiation-absorbed dose to tumor compared with the intact mAb, but reduce the radiation absorbed dose to bone marrow. In addition, low or variable expression of tumor-associated target antigens or receptors may lead to low or heterogeneous tumor uptake of radiolabeled mAbs. This report also discusses a novel approach toward systemic radiotherapy that combines gene transfer techniques (to increase tumor receptor expression) with radiolabeled peptides that target the induced receptor. The radiolabeled peptides achieve good tumor uptake, rapid tumor penetration, and rapid blood clearance.

A humanized construct of the CC49 (HuCC49) high-affinity anti-TAG-72 mAb, as well as a construct with the CH2 region deleted (HuCC49ΔCH2), were labeled with ^{131}I and ^{177}Lu. Biodistribution of the radiolabeled constructs was evaluated 24 h after regional i.p. injection in athymic nude mice bearing i.p. LS174T human colon cancer xenografts. The ^{131}I-HuCC49ΔCH2 showed a median tumor uptake of 5.5% ID/g which was similar to that of ^{131}I-HuCC49 at 5.2% ID/g. However, the median blood concentration of ^{131}I-HuCC49ΔCH2 was 0.2% ID/g which was significantly lower than 0.8% ID/g for ^{131}I-HuCC49. The uptake of the constructs in other normal tissues were similar. The ^{177}Lu-HuCC49ΔCH2 showed a median tumor uptake of 9.4% ID/g, which was slightly higher than that of ^{177}Lu-HuCC49 at 7.9% ID/g. The median blood concentration of ^{177}Lu-HuCC49ΔCH2 was 0.2% ID/g, which was significantly lower than 0.4% ID/g for ^{177}Lu-HuCC49. The uptake of the antibody constructs in other normal tissues were similar except for the kidney. The tumor:blood ratios of ^{177}Lu-HuCC49 and ^{177}Lu-HuCC49ΔCH2 were 19.4 and 60.2, respectively, at 24 h after injection.

The purpose of the second aspect of the study was to determine the biodistribution of ^{64}Cu-1,4,8,11-tetraazacyclotetradecane-1,4,8,11-tetraacetic acid (TETA)-octreotide in a human ovarian cancer model induced to express human somatostatin receptor subtype 2 (SSTr2) using gene transfer techniques as a prelude to future therapy studies. Mice bearing i.p. SKOV3.ip1 tumors transduced with an adenoviral vector encoding the cDNA for SSTr2 (*AdSSTr2*) and injected i.p. with ^{64}Cu-TETA-octreotide showed a median uptake of 24.3% ID/g in tumor at 4 h postinjection compared with 4.9% ID/g at 18 h after injection. Also, tumor uptake of ^{64}Cu-TETA-octreotide at 4 h was not significantly different when administered either 2 or 4 days after injection of *AdSSTr2* ($P = 0.076$). ^{64}Cu-TETA-octreotide should be useful for targeted radiotherapy against tumors that are genetically induced to express high levels of SSTr. These two novel targeting strategies show promise for improved cancer radioimmunotherapy.

Introduction

Limitations of RIT[3] reflect a variety of problems that include: (*a*) inadequate expression of tumor-associated antigens or receptors; (*b*) variable expression of target receptor; (*c*) poor tumor penetration of high-molecular-weight mAbs used to deliver radionuclides to the tumor; (*d*) a humoral immune response

[1] Presented at the "Seventh Conference on Radioimmunodetection and Radioimmunotherapy of Cancer," October 15–17, 1998, Princeton, NJ. This work was supported by NIH Grants R01 CA 73636, R01 CA 62550, and R01 CA 78505 (to D. J. B.), NIH Grants R01 CA 68245 and R01 CA 74242 (to D. T. C.), and Department of Energy Grant DE-FG05-93ER61654 (to D. J. B.).

[2] To whom requests for reprints should be addressed, at Department of Radiation Oncology, University of Alabama at Birmingham, 1824 6th Avenue South, WTI 674, Birmingham, AL 35294. Phone: (205) 934-7077; Fax: (205) 975-7060; E-mail: djb@uab.edu.

[3] The abbreviations used are: RIT, radioimmunotherapy; BSM, bovine submaxillary mucin; HPLC, high-pressure liquid chromatography; SSTr2, human somatostatin receptor subtype 2; *AdSSTr2*, recombinant adenoviral vector-encoding gene for SSTr2; % ID/g, percent injected dose per gram of tissue; TETA, 1,4,8,11-tetraazacyclotetradecane-1,4,8,11-tetraacetic acid; mAb, monoclonal antibody; pfu, plaque-forming unit(s); GRITS, genetic radioisotope targeting strategies; PA-DOTA, 1,4,7,10-tetraaza-*N*-(1-carboxy-3-(4 nitrophenyl)propyl)-*N*′, *N*′′, *N*′′′-tris(acetic acid) cyclododecane; PA-DOTA-NCS, 1,4,7,10-tetraaza-*N*-(1-carboxy-3-(4-isothiocyanatophenyl)propyl)-*N*′, *N*′′, *N*′′′-tris(acetic acid) cyclododecane.

against the mAbs; and (*e*) bone marrow toxicity resulting from the slow blood-clearance of radiolabeled mAbs (1–6). A strategy to overcome these problems has been the use of radiolabeled mAb fragments or peptides that clear faster from the blood and show more rapid and homogeneous intratumor distribution (2, 3, 6).

Murine CC49 has an excellent binding affinity for TAG-72, and this antigen is quite plentiful in many human adenocarcinomas (7). The CC49 molecule was changed to a "humanized" construct using complementarity-determining region (CDR) grafting techniques. This should reduce immunogenicity and allow more than one treatment course to be given. However, construction of antibodies with human constant regions (chimeric or CDR-grafted molecules) results in a substantial increase in their half-life in plasma (8), and this prolonged radiation exposure of the marrow reduces the maximum tolerated dose and limits the dose administered (9). This is true for i.p. as well as for i.v. administration because the majority of the dose administered into the peritoneal cavity eventually enters the plasma compartment. It has been shown that the deletion of the CH2 region of the molecule results in dramatic shortening of plasma half-life with retention of binding affinity and tumor localization (10). Animal model studies have confirmed the predicted behavior of this new humanized antibody construct, including improved tumor:blood ratios. We believe that this antibody molecule will be ideal for i.p. RIT in that its rapid clearance from the plasma and prompt excretion should provide a higher maximum tolerated dose and, thus, a higher dose that can be delivered while retaining its regional tumor localization capacity. Furthermore, its reduced immunogenicity will allow two or more courses of therapy, which should enhance antitumor effects as well.

Another strategy to increase the tumor localization of radiolabeled mAbs or peptides has been through the genetic induction of antigens and receptors, termed GRITS (11–17). This strategy addresses the problem of inadequate tumor-associated antigens or receptors by increasing their concentration through gene transfer methods. This increase in antigen or receptor concentration results in an increase in the targets for the radiolabeled mAb or peptide at the tumor site and, hence, a higher binding of either by the tumor. We have been investigating the SSTr2/octreotide system. Octreotide is an eight-amino-acid derivative of the inhibitory peptide somatostatin, which binds with highest affinity to SSTr2 (18). Octreotide analogues radiolabeled with ^{90}Y, ^{188}Re, and ^{64}Cu have demonstrated therapeutic efficacy in animal models (19–22).

In the present study, it is also shown that a replication-incompetent adenoviral vector that encodes the *SSTr2* gene driven by the cytomegalovirus promoter (*AdSSTr2*) can mediate the expression of SSTr2 in human tumor cell lines *in vitro* using a competitive binding assay with ^{64}Cu-TETA-octreotide as the radioligand. The *AdSSTr2* was then used to induce the expression of SSTr2 in a mouse model of human ovarian carcinoma as demonstrated by tumor localization of ^{64}Cu-TETA-octreotide. ^{64}Cu has an appropriate physical half-life (12.8 h) to match the biological half-life of octreotide retention in tumors (27.1 h) and can achieve effective cell-kill over several cell diameters.

Materials and Methods

Cell Line and Antibodies. The LS174T human colon cancer cell line was obtained from the American Type Culture Collection (Manassas, VA) and cultured in Eagle's MEM containing 10% fetal bovine serum, 1% L-glutamine, and 1% nonessential amino acids at 37°C in a humidified atmosphere with 5% CO_2. The HuCC49 and HuCC49ΔCH2 mAbs were prepared as described previously (23, 24) and stored at −70°C until use.

Radiolabeling of Antibodies with ^{131}I. HuCC49 and HuCC49ΔCH2 were labeled with $Na^{131}I$ (DuPont NEN Research Products, Boston, MA; specific activity = 630 Ci/mmol) using the IodoGen (Pierce Chemical Co., Rockford, IL) method (25). The reaction products were purified using a PD-10 column (Pharmacia, Piscataway, NJ). The purity of the radiolabeled mAbs was determined by size-exclusion HPLC. HPLC samples were run on a Hydropore SEC 83-S13-C5 column (Rainin Instrument Co., Woburn, MA) using a Bio-Rad HPLC Pump Model 1330 (Bio-Rad Laboratories, Hercules, CA) and an isocratic buffer of 10 mM Na_2HPO_4, 300 mM NaCl, and 10% DMSO at a flow rate of 1 ml/min.

Radiolabeling of Antibodies with ^{177}Lu. The bifunctional chelating agent PA-DOTA-NCS was synthesized as described previously (26) and conjugated to HuCC49 and HuCC49ΔCH2. Briefly, the PA-DOTA-NCS was diluted to 0.5 mg/ml in 0.1 M H_3BO_4 and added to HuCC49 and HuCC49ΔCH2 (in the same buffer) in a 4.5:1 molar ratio such that the final concentration of HuCC49 and HuCC49ΔCH2 were ~10 μM. The reaction mixtures were then incubated at 37°C for 4 h and purified using a Centricon 30 concentrator (Amicon Inc., Beverly, MA) The samples were added to the Centricon 30, diluted to 2.0 ml with 0.1 M NH_4OAc (pH 5.5), and centrifuged. This was repeated three times, the conjugates collected, and stored at 4°C until needed. $^{177}LuCl_3$ (initial specific activity = ~4,000 Ci/mmol) was produced and purified at the University of Missouri-Columbia Research Reactor. The $^{177}LuCl_3$ was converted to ^{177}Lu-acetate using a 10-fold dilution with 0.1 M NH_4OAc (pH 5.5) and was added to the PA-DOTA-NCS conjugates. The reaction mixtures were incubated for 30 min at 37°C and purified using a BioSpin 6 chromatography column (Bio-Rad Laboratories) equilibrated with 0.1 M NH_4OAc (pH 5.5). The purity of the radiolabeled conjugates was determined by size-exclusion HPLC as described above.

Immunoreactivity Assay of Radiolabeled Antibodies. The immunoreactivity of radiolabeled antibody preparations was measured using BSM (Sigma Chemical, St. Louis, MO) coated beads. The BSM was immobilized onto a solid support (6.2-mm polystyrene beads, Precision Plastic Ball, Franklin Park, IL) at a concentration of 10 μg of BSM per bead. The radiolabeled mAbs were prepared at 10 ng/ml in 1% BSA in PBS and added in duplicate (100 μl) to a 12 × 75-mm glass test tube containing a single BSM bead in the absence and presence of increasing concentrations of unlabeled mAb. The tubes were counted in a gamma scintillation counter and incubated for 1 h at room temperature over a laboratory oscillator. The BSM beads were washed with 4 ml of PBS, and the radioactivity remaining in each tube was measured. The total percent radioactivity bound to the BSM beads was calculated, and the inverse of % binding was plotted *versus* the inverse of the concentration

of unlabeled mAbs. The inverse of the Y-intercept was determined as % immunoreactive fraction.

Radiolabeled Antibody Biodistribution Studies. BALB/c athymic nude mice (National Cancer Institute Frederick Research Laboratory, Frederick, MD) were implanted i.p. with 1×10^8 LS174T cells followed by an i.p. injection of 2 μCi of ^{131}I-HuCC49 or ^{131}I-HuCC49ΔCH2 8 days later. The mice were then killed 24 h after the injection of the radiolabeled antibodies. The tumor, blood, kidney, liver, spleen, heart, lung, stomach, small intestine, skin, bone, peritoneal lining, uterus, pancreas, and muscle were removed and weighed, and the activity was counted in a gamma counter. Similarly, mice were given injections i.p. of 2 μCi of ^{177}Lu-PA-DOTA-HuCC49 or ^{177}Lu-PA-DOTA-HuCC49ΔCH2 8 days after tumor cell inoculation and were killed 24 h after the injection of the radiolabeled antibodies. The tissues were harvested and counted as described above.

Radiolabeling of TETA-Octreotide with ^{64}Cu. TETA (Aldrich Chemical Co., Milwaukee, WI) was conjugated to octreotide as described previously (27). $^{64}CuCl_2$ (initial specific activity = ~5,000 Ci/mmol) was produced and purified at the University of Missouri-Columbia Research Reactor and was used to label TETA-octreotide as described previously (27). Briefly, the TETA-octreotide was mixed with ^{64}Cu-acetate in 0.1 M NH_4OAc buffer (pH 5.5) and was incubated at room temperature for 1 h. Gentisic acid (1 mg/ml) was added to the mixture to reduce the effects of radiolysis. Reaction products were purified using a C-18 SepPak. The mixture was added to the SepPak, rinsed with 5 ml of 0.1 M NH_4OAc (pH 5.5) to remove uncomplexed ^{64}Cu, and rinsed with ethanol to elute the ^{64}Cu-TETA-octreotide product. Purity was confirmed by reverse-phase HPLC and TLC.

Competitive Binding Assay. A427 lung and SKOV3.ip1 ovarian cancer cells were maintained in DMEM containing 10% fetal bovine serum, were cultured at 37°C in a humidified atmosphere with 5% CO_2, and were seeded so that they were ~80% confluent at the time they were infected. The A427 cells were infected at 0 and 10 pfu/cell with *AdSSTr2*, whereas the SKOV3.ip1 cells were infected with 0 and 100 pfu/cell of *AdSSTr2* because they are less easily transduced (16). The cells were grown for 48 h and then were harvested to form membrane preparations as described previously (16). The membrane preparations were then diluted with buffer [10 mM HEPES, 5 mM $MgCl_2$, 1 mM EDTA, 0.1% BSA, 10 μg/ml leupeptin, 10 μg/ml pepstatin, 0.5 μg/ml aprotinin, and 200 μg/ml bacitracin (pH 7.4)] to 0.5 mg/ml. One hundred μl (50 μg) of membrane preparation were added to Multiscreen Durapore filtration plates (type FB, 1.0-μm borosilicate glass fiber over 1.2-μm Durapore membrane, Millipore, Bedford, MA) in triplicate and washed with buffer [10 mM HEPES, 5 mM $MgCl_2$, 1 mM EDTA, and 0.1% BSA (pH 7.4)]. One hundred μl of ^{64}Cu-TETA-octreotide (0.05 nM) were added to each well and were incubated for 90 min at room temperature. The samples were then washed twice with ice-cold buffer, the filters were allowed to dry, and the individual wells were punched out and counted in a gamma counter. Nonspecific binding was assessed using a 1000-fold molar excess of octreotide to inhibit the binding of ^{64}Cu-TETA-octreotide.

^{64}Cu-TETA-Octreotide Biodistribution Studies. Biodistribution studies were performed in groups of 5 athymic nude mice bearing i.p. SKOV3.ip1 tumors. SKOV3.ip1 cells (2×10^7) were injected i.p. into the mice. After 5 days, *AdSSTr2* (1×10^9 pfu) was injected i.p. followed by the i.p. administration of ^{64}Cu-TETA-octreotide (2 μCi) 2 days later. The animals were killed 4 or 18 h after the injection of the radiolabeled peptide; the blood, lungs, liver, small intestine, spleen, kidney, bone, pancreas, tumor, peritoneal lining, and uterus were removed and weighed, and the radioactivity was counted in a gamma counter. Also, in a separate experiment, mice received 1×10^9 pfu of a control adenovirus (*AdLacZ*) or 1×10^9 pfu of *AdSSTr2* to demonstrate the specificity of ^{64}Cu-TETA-octreotide localization. In another experiment, ^{64}Cu-TETA-octreotide was administered 2 or 4 days after *AdSSTr2* injection followed by the killing of the animals 4 h after the injection of the radiolabeled peptide. A pharmacokinetic analysis was also performed by administering ^{64}Cu-TETA-octreotide 2 days after the *AdSSTr2* injection, then killing the mice at 30 min and 2, 4, 6, 16, 18, 24, and 36 h later, and counting the tissues in a gamma counter. The tumors were approximately 0.1 g in size and consisted of one nodule with no visible ascites.

Statistical Analysis. The Wilcoxon rank-sum test was used to compare the uptake of radiolabeled HuCC49 and HuCC49ΔCH2 antibody in tumor and normal tissues as well as the tumor:blood ratios for both ^{131}I- and ^{177}Lu-labeled antibodies. The Wilcoxon signed-rank test was used to compare the amount of ^{64}Cu-TETA-octreotide uptake within tissues in the various studies. The median localization as well as the 25th and 75th percentile were used to summarize the central tendency and variability for each tissue, by group, for each experiment.

Results

Radiolabeling of mAbs and Immunoreactivity. The specific activities of HuCC49 and HuCC49ΔCH2 labeled with ^{131}I were both ~6 mCi/mg. The specific activities of ^{177}Lu-PA-DOTA-HuCC49 and ^{177}Lu-PA-DOTA-HuCC49ΔCH2 were both ~0.6 mCi/mg. All of the radiolabeled conjugates were shown to be >95% pure by gel-filtration-size exclusion HPLC. The immunoreactivity of ^{131}I-HuCC49 and ^{131}I-HuCC49ΔCH2 were both ~67%. The immunoreactivity of the ^{177}Lu-HuCC49 conjugate was 45%, compared with 35% for the ^{177}Lu-HuCC49ΔCH2 conjugate.

Biodistribution Studies of Radiolabeled MAbs. The tumor localization and biodistribution of ^{131}I- or ^{177}Lu-labeled HuCC49 and HuCC49ΔCH2 were determined in groups of 4–5 athymic nude mice bearing LS174T human colon i.p. tumor nodules (0.1–0.4 g) at 24 h after injection (Tables 1 and 2). The median tumor concentrations for ^{131}I- and ^{177}Lu-HuCC49 and ^{131}I- and ^{177}Lu-HuCC49ΔCH2 were 5.2, 7.9, 5.5, and 9.4% ID/g, respectively (Tables 1 and 2), and did not differ ($P = 0.16$). The respective blood concentrations for ^{131}I-HuCC49 and ^{131}I-HuCC49ΔCH2 were 0.8 and 0.2% ID/g ($P = 0.016$), whereas the respective blood concentrations for ^{177}Lu-HuCC49 and ^{177}Lu-HuCC49ΔCH2 were 0.4 and 0.2% ID/g ($P = 0.016$). The tumor:blood ratios for ^{177}Lu-HuCC49 and ^{177}Lu-HuCC49ΔCH2 were 19.4 and 60.2, respectively ($P = 0.016$), whereas the tumor:blood ratios for ^{131}I-HuCC49

Table 1 Biodistribution of ^{131}I-HuCC49 and ^{131}I-HuCC49ΔCH2 labeled by the IodoGen technique in groups of four to five athymic nude mice bearing i.p. LS174T human colon cancer xenografts at 24 h after i.p. injection

Tissue	^{131}I-HuCC49[a] (% ID/g)	^{131}I-HuCC49ΔCH2[b] (% ID/g)	P[c]
Tumor	5.2 (2.7–7.3)	5.5 (4.0–5.5)	1.000
Blood	0.8 (0.7–0.9)	0.2 (0.2–0.2)	0.016
Kidney	0.6 (0.5–0.7)	0.6 (0.3–0.6)	0.413
Liver	10.7 (8.4–11.5)	8.4 (3.5–15.1)	0.905
Spleen	1.5 (1.1–1.9)	1.5 (0.8–1.6)	0.976
Heart	0.3 (0.3–0.3)	0.1 (0.1–0.2)	0.079
Lung	1.0 (0.5–1.6)	0.5 (0.3–1.2)	0.556
Stomach	1.7 (1.5–1.7)	1.6 (1.6–1.9)	1.000
Small intestine	0.4 (0.3–0.6)	0.4 (0.3–0.5)	0.905
Skin	0.4 (0.4–0.4)	0.2 (0.2–0.2)	0.016
Bone	0.4 (0.4–0.5)	0.7 (0.4–1.0)	0.318
Peritoneal lining	2.1 (1.0–3.0)	1.5 (0.4–3.2)	1.000
Uterus	2.6 (1.8–3.9)	2.5 (2.2–4.1)	0.905
Pancreas	1.5 (1.4–2.0)	2.7 (2.2–3.1)	0.286
Muscle	0.2 (0.2–0.3)	0.2 (0.2–0.2)	0.389

[a] Median with interquartile range in parentheses for four mice.
[b] Median with interquartile range in parentheses for five mice.
[c] Comparison of ^{131}I-HuCC49 *versus* ^{131}I-HuCC49ΔCH2 via Wilcoxon rank-sum test.

Table 2 Biodistribution of ^{177}Lu-PA-DOTA-HuCC49 and ^{177}Lu-PA-DOTA-HuCC49ΔCH2 in groups of four to five athymic nude mice bearing i.p. LS174T human colon cancer xenografts at 24 h after i.p. injection

Tissue	^{177}Lu-HuCC49[a] (% ID/g)	^{177}Lu-HuCC49ΔCH2[b] (% ID/g)	P[c]
Tumor	7.9 (6.6–9.3)	9.4 (5.8–14.3)	0.905
Blood	0.4 (0.3–0.5)	0.2 (0.1–0.2)	0.016
Kidney	2.2 (1.9–2.2)	5.8 (4.5–9.3)	0.016
Liver	6.4 (4.3–7.2)	9.2 (5.6–19.0)	0.730
Spleen	1.8 (1.4–2.9)	4.0 (2.5–8.5)	0.191
Heart	0.5 (0.4–0.6)	0.5 (0.4–0.7)	0.952
Lung	1.2 (1.2–1.8)	0.9 (0.8–1.4)	0.191
Stomach	1.2 (1.1–1.2)	0.6 (0.5–0.9)	0.167
Small intestine	0.6 (0.6–0.7)	0.9 (0.4–1.5)	1.000
Skin	0.5 (0.4–0.5)	0.3 (0.2–0.5)	0.286
Bone	1.7 (1.4–1.8)	2.2 (1.1–4.5)	0.730
Peritoneal lining	9.9 (6.4–10.3)	10.0 (8.1–14.5)	0.413
Uterus	3.3 (3.1–3.7)	4.2 (2.7–6.3)	0.556
Pancreas	3.8 (2.4–3.8)	4.7 (3.9–5.9)	0.191
Muscle	0.5 (0.4–0.6)	0.4 (0.3–0.5)	0.373

[a] Median with interquartile range in parentheses for five mice.
[b] Median with interquartile range in parentheses for four mice.
[c] Comparison of ^{177}Lu-HuCC49 *versus* ^{177}Lu-HuCC49ΔCH2 via Wilcoxon rank-sum test.

and ^{131}I-HuCC49ΔCH2 were 6.2 and 27.4, respectively (P = 0.016). The uptake of ^{131}I-HuCC49 and ^{131}I-HuCC49ΔCH2 in kidney (0.6 and 0.6% ID/g), liver (10.7 and 8.4% ID/g), spleen (1.5 and 1.5% ID/g), and other normal tissues were similar ($P > 0.079$), except for skin (0.4 and 0.2% ID/g). The uptake of ^{177}Lu-HuCC49ΔCH2 in kidney (5.8% ID/g) was higher than for ^{177}Lu-HuCC49 (2.2% ID/g; P = 0.016), whereas the uptake in liver (9.2 and 6.4% ID/g, respectively) and spleen (4.0 and 1.8% ID/g, respectively) of the two mAbs were similar (P = 0.730 and P = 0.191, respectively). In a repeat study, the kidney uptake of ^{177}Lu-HuCC49ΔCH2 (3.0% ID/g) was lower than ^{177}Lu-HuCC49 (5.7% ID/g) at 24 h after injection (data not shown). Our hypothesis is that the difference may have been due to a different PA-DOTA:mAb molar ratio. The uptake in other normal tissues of ^{177}Lu-HuCC49 and ^{177}Lu-HuCC49ΔCH2 did not differ (Table 2). Furthermore, as determined by immunohistology, the intratumor distribution of the HuCC49ΔCH2 was much more uniform than the surface distribution of HuCC49 at 4 h after injection.[4]

Competitive Binding Assay. Membrane preparations from A427 cells infected with 10 pfu/cell *AdSSTr2* or from SKOV3.ip1 cells infected with 100 pfu/cell *AdSSTr2* demonstrated 37% and 20% binding, respectively, of ^{64}Cu-TETA-octreotide, compared with <1.0% binding with uninfected cells or infected cells blocked with an excess of unlabeled octreotide (Fig. 1).

^{64}Cu-TETA-Octreotide Biodistribution Studies. Tumor localization and pharmacokinetics of ^{64}Cu-TETA-octreotide was investigated in mice bearing i.p. SKOV3.ip1 human ovarian tumors induced to express SSTr2 with *AdSSTr2*. Mice bearing i.p. SKOV3.ip1 tumors infected with 1×10^9 pfu *AdSSTr2* or *AdLacZ* 5 days after tumor cell inoculation, followed by i.p. injection of ^{64}Cu-TETA-octreotide 2 days later, had median (25–75th percentile range) tumor uptakes of 11.4 (range, 7.6–17.0) % ID/g and 1.6 (range, 1.6–1.8) % ID/g, respectively (P = 0.002), at 4 h after ^{64}Cu-TETA-octreotide administration (Fig. 2). A larger uptake of ^{64}Cu-TETA-octreotide was also observed in the liver, small intestine, spleen, peritoneal lining, uterus, and pancreas of mice that received *AdSSTr2* compared with mice given *AdLacZ*. This may be due to *AdSSTr2* infection of these organs. Mice given *AdSSTr2* had tumor:blood, tumor:kidney, and tumor:liver ratios of 27.3, 2.7, and 2.2, respectively, at 4 h after ^{64}Cu-TETA-octreotide administration. Mice given ^{64}Cu-TETA-octreotide 2 or 4 days after i.p. injection of *AdSSTr2* had similar median tumor uptake of 11.2 (10.6–12.9) % ID/g and 16.4 (12.7–27.4) % ID/g, respectively (P = 0.076), 4 h later (Fig. 3). Other normal tissues also demonstrated similar uptake except for the blood, lung, liver, and bone, which had significantly greater uptake 4 days after *AdSSTr2* administration than 2 days after administration ($P <$ 0.032). In a separate experiment, mice killed 4 or 18 h after the injection of ^{64}Cu-TETA-octreotide showed a median tumor uptake of 24.3 (17.0–31.1)% ID/g at 4 h, which decreased to 4.9 (2.9–8.0)% ID/g at 18 h (Fig. 4). Pharmacokinetic analysis demonstrated that clearance of ^{64}Cu-TETA-octreotide from the tumor, blood, liver, and kidney was best fit using a two-compartment model. The radioactivity cleared from a tumor with an α half-life of 1.2 h and a β half-life of 27.1 h. In contrast, blood demonstrated an initial clearance half-life of 0.3 h followed by the accumulation of radioactivity with a doubling time of 46.2 h. These studies demonstrated that ^{64}Cu-TETA-octreotide localized in human ovarian tumors that were induced to express SSTr2 with *AdSSTr2 in vivo*. In addition, ^{64}Cu-TETA-octreotide has been demonstrated to be useful in therapy studies, which indicates that it should have therapeutic efficacy in this human

[4] B. E. Rogers and D. J. Buchsbaum, unpublished observations.

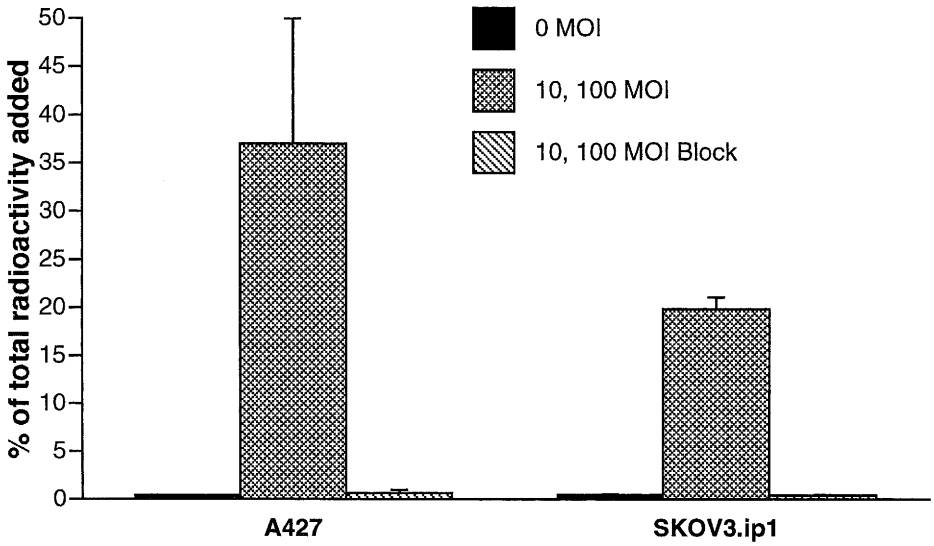

Fig. 1 Binding of ^{64}Cu-TETA-octreotide to A427 and SKOV3.ip1 membrane preparations from cells that were either uninfected or infected with 10 or 100 pfu/cell *AdSSTr2*. A427 cells were infected with 10 pfu/cell, whereas SKOV3.ip1 cells were infected with 100 pfu/cell. Binding to infected cells was blocked using a 1000-fold molar excess of unlabeled octreotide. *Bar*, the mean amount of ^{64}Cu-TETA-octreotide bound as a percentage of total radioactivity added ± SD ($n \geq 6$).

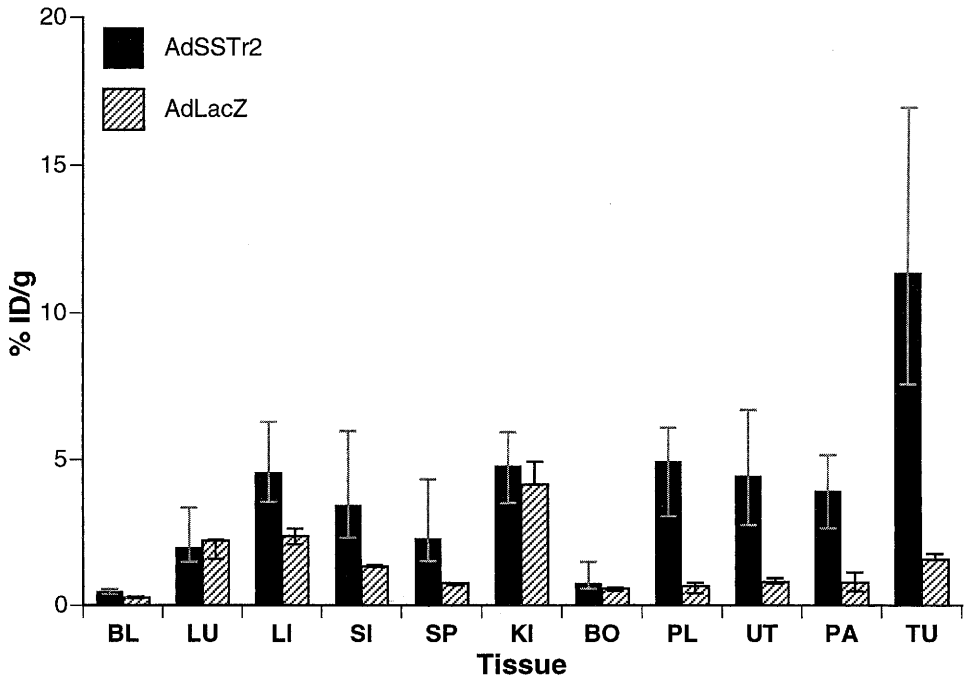

Fig. 2 Biodistribution of ^{64}Cu-TETA-octreotide in nude mice inoculated with 2×10^7 SKOV3.ip1 human ovarian cancer cells i.p. Five days after tumor cell inoculation, *AdSSTr2* or *AdLacZ* was injected i.p., followed by i.p. administration of ^{64}Cu-TETA-octreotide 2 days later. Four h after radioligand injection, groups of mice were killed, and the organs were harvested and counted in a gamma counter. *BL*, blood; *LU*, lung; *LI*, liver; *SI*, small intestine; *SP*, spleen; *KI*, kidney; *BO*, bone; *PL*, peritoneal lining; *UT*, uterus; *PA*, pancreas; *TU*, tumor. *B*ar, the median tissue concentration from a group of five animals with a range from the 25th to the 75th percentile.

ovarian cancer model induced to express SSTr2 because of its high uptake in tumor and its comparable biological half-life in tumor (27.1 h) with the physical half-life of ^{64}Cu (12.8 h).

Discussion

Problems regarding the slow clearance of radiolabeled intact mAbs from the blood and their inability to rapidly penetrate solid tumors needed to be addressed. Therefore, our group has focused on the use of a CH2 domain-deleted mAb, which clears more rapidly from blood than intact mAb. The biodistribution data indicate that the use of HuCC49ΔCH2 antibody results in similar high i.p. tumor binding after i.p. injection relative to HuCC49 antibody, but a much more rapid clearance from blood resulting in a substantially greater tumor:blood ratio. This was true for the HuCC49ΔCH2 labeled with both ^{131}I and ^{177}Lu. These data suggest that the CH2 domain-deleted antibody will be more therapeutically efficacious than the intact mAb in future therapy studies.

The tumor uptake of the ^{177}Lu-labeled mAbs may be improved further by increasing their immunoreactivity. This may be accomplished by adjusting the PA-DOTA-NCS to mAb molar ratio. It is likely that the antigen-binding site of the mAbs was damaged with PA-DOTA-NCS by using the 4.5:1 molar

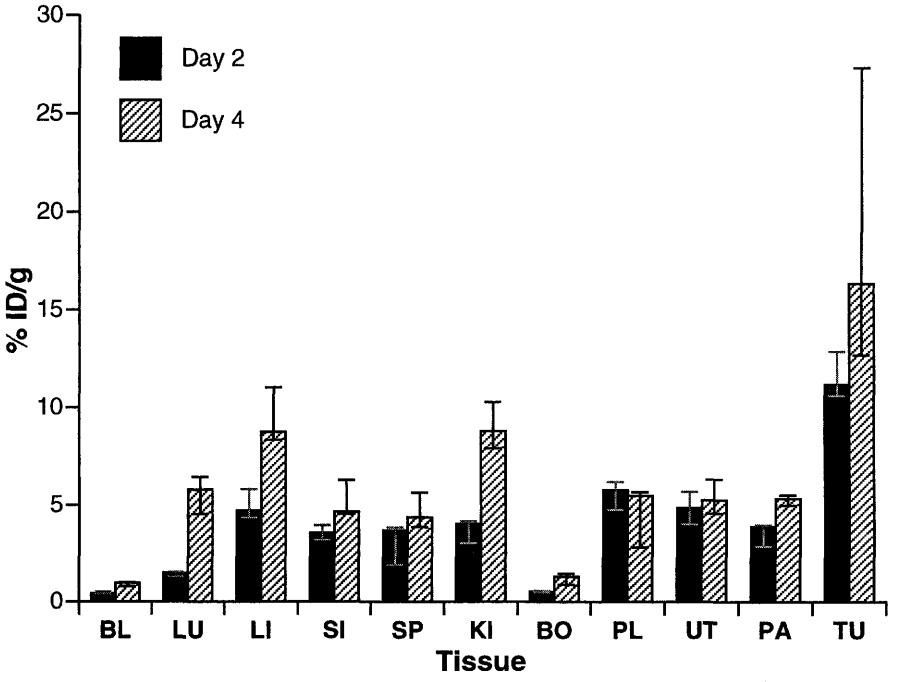

Fig. 3 Biodistribution of ^{64}Cu-TETA-octreotide in nude mice inoculated with 2×10^7 SKOV3.ip1 human ovarian cancer cells i.p. Five days after tumor cell inoculation, *AdSSTr2* was injected i.p., followed by i.p. administration of ^{64}Cu-TETA-octreotide 2 or 4 days later. Four h after radioligand injection, groups of mice were killed, and the organs were harvested and counted in a gamma counter. *Bar*, the median tissue concentration from a group of five animals with a range from the 25th to the 75th percentile. Abbreviations are defined in Fig. 2.

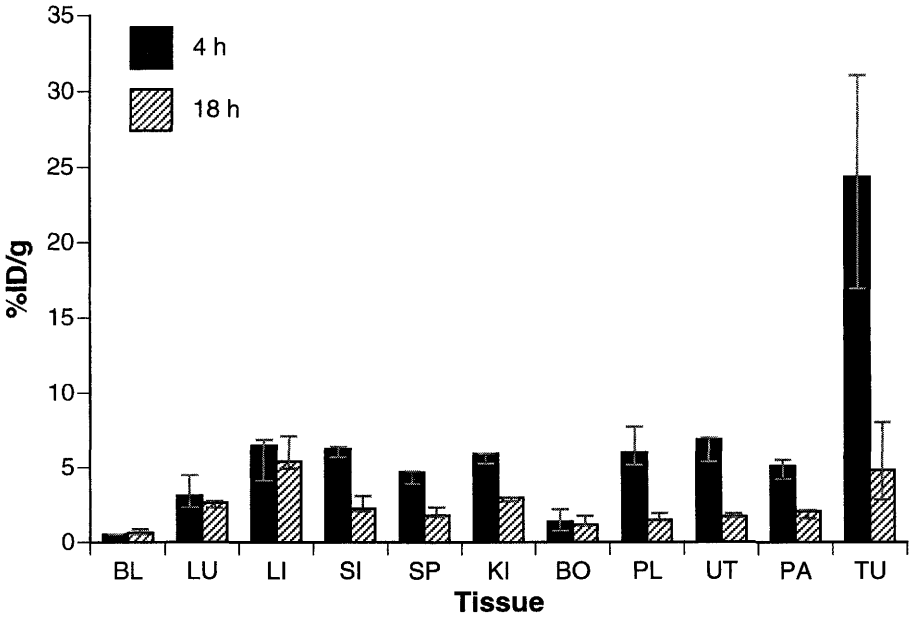

Fig. 4 Biodistribution of ^{64}Cu-TETA-octreotide in nude mice inoculated with 2×10^7 SKOV3.ip1 human ovarian cancer cells i.p. Five days after tumor cell inoculation, *AdSSTr2* was injected i.p., followed by i.p. administration of ^{64}Cu-TETA-octreotide 2 days later. Four and 18 h after radioligand injection, groups of mice were killed, and the organs were harvested and counted in a gamma counter. *Each bar*, the median tissue concentration from a group of 5–15 animals with a range from the 25th to the 75th percentile. Abbreviations are defined in Fig. 2.

ratio described. Lowering this ratio to 1:1 increased the immunoreactivities of the mAbs to 55–60% and did not significantly decrease the radiolabeling efficiencies (data not shown). The median tumor uptake of ^{131}I-HuCC49 and ^{131}I-HuCC49ΔCH2 were 5.2 and 5.5% ID/g, respectively (Table 1). Previous studies have not investigated the tumor uptake of radioiodinated HuCC49 and HuCC49ΔCH2 injected i.p. into mice bearing i.p. LS174T tumors. Slavin-Chiorini *et. al.* (24) investigated the tumor uptake of radioiodinated HuCC49 and HuCC49ΔCH2 injected either i.p. or i.v into mice bearing s.c. LS174T tumors. They showed tumor uptake of radioiodinated HuCC49 and HuCC49ΔCH2 of 9.0 and 11.1% ID/g, respectively, after i.v. injection and 5.8 and 5.4% ID/g, respectively, after i.p. injection. Comparison of these results to those obtained in this study are difficult because of the different animal models used (i.p. *versus.* s.c. LS174T tumors).

We also have focused on using adenoviral vectors to increase the expression of target receptors on tumors. These

receptors can then be targeted with radiolabeled peptides, which should overcome the problems associated with the intact radiolabeled mAbs discussed above. In the present study, we found that *AdSSTr2* can mediate the expression of SSTr2 in human tumor cell lines *in vitro* using a competitive binding assay with ^{64}Cu-TETA-octreotide as the radioligand. Previously, we reported that *AdSSTr2*-infected A427 and SKOV3.ip1 cells express SSTr2 at ~1000 and ~150 fmol/mg membrane preparation, respectively (16). In addition, Anderson *et al.* (20, 27) demonstrated that ^{64}Cu-TETA-octreotide binds with high affinity to SSTr2-expressing cells. The *AdSSTr2* was then used to induce the expression of SSTr2 in a mouse model of human ovarian carcinoma. This demonstrated good tumor uptake of ^{64}Cu-TETA-octreotide (11.4% ID/g) compared with the results when the control *AdLacZ* virus was given (1.6% ID/g; Fig. 2). However, there was also normal tissue uptake of ^{64}Cu-TETA-octreotide after the injection of *AdSSTr2*. This could be due to the transduction of tumor that metastasized to these tissues or the transduction of these tissues with *AdSSTr2*. The latter problem may be overcome by using adenoviral "targeting" strategies discussed below. It was also shown that the tumor uptake of ^{64}Cu-TETA-octreotide at 4 h was similar at both 2 and 4 days after *AdSSTr2* injection (Fig. 3). This is significant because it illustrates that fractionated doses of ^{64}Cu-TETA-octreotide can be administered over a 2–4 day period after *AdSSTr2* injection. Finally, the retention of ^{64}Cu-TETA-octreotide in the tumor over time is illustrated in Fig. 4 and by the pharmacokinetic results which show that the ^{64}Cu-TETA-octreotide remained in the tumor long enough (β half-life = 27.1 h) to achieve good dose deposition from the short-lived ^{64}Cu (12.8 h).

The GRITS approach can potentially be improved upon by targeting adenoviral vectors specifically to tumor cells so that the transduced receptor is not expressed on normal tissues. This would result in higher tumor:normal tissue radiolabeled peptide-uptake ratios. Limiting receptor expression to tumor sites can be accomplished by retargeting vectors to tumor-specific receptors (transductional targeting) via genetic or immunological methods (28–36), which can result in increased gene transfer (30, 32–34), or by using tumor-specific regulatory sequences to control gene expression after viral infection (transcriptional targeting; Ref. 37).

Of key interest are the findings that radiolabeled HuCC49ΔCH2 and octreotide had higher tumor:blood ratios and shorter half-lives in blood than radiolabeled antibodies, which should result in less bone marrow toxicity than experienced with radiolabeled antibodies. It is important to note that the high tumor uptake of the radiolabeled octreotide resulted from the use of a novel gene transfer strategy to induce high levels of somatostatin receptor on the tumor cells. Because of the high tumor uptake and the much more rapid clearance from blood of specific radiolabeled CH2 domain-deleted mAbs and octreotide compared with intact mAbs, these novel targeting strategies show promise for improved cancer RIT.

Acknowledgments

We thank Sally Lagan for help in preparation of the manuscript. The radioiodinations were performed at the University of Alabama-Birmingham Comprehensive Cancer Center Core Facility. We acknowledge Stephanie McLean, Kim Laffoon, Richard Kirkman, Sheila Bright, Christine Olsen, and Christy Grimes for expert technical assistance.

References

1. Philben, V. J., Jakowatz, J. G., Beatty, B. G., Vlahos, W. G., Paxton, R. J., Williams, L. E., Shively, J. E., and Beatty, J. D. The effect of tumor CEA content and tumor size on tissue uptake of Indium 111-labeled anti-CEA monoclonal antibody. Cancer (Phila.), *57:* 571–576, 1986.

2. Fujimori, K., Covell, D. G., Fletcher, J. E., and Weinstein, J. N. Modeling analysis of the global and microscopic distribution of immunoglobulin G, F(ab′)$_2$, and Fab in tumors. Cancer Res., *49:* 5656–5663, 1989.

3. Yokota, T., Milenic, D. E., Whitlow, M., and Schlom, J. Rapid tumor penetration of a single-chain Fv and comparison with other immunoglobulin forms. Cancer Res., *52:* 3402–3408, 1992.

4. Shockley, T. R., Lin, K., Sung, C., Nagy, J. A., Tompkins, R. G., Dedrick, R. L., Dvorak, H. F., and Yarmush, M. L. A quantitative analysis of tumor specific monoclonal antibody uptake by human melanoma xenografts: effects of antibody immunological properties and tumor antigen expression levels. Cancer Res., *52:* 357–366, 1992.

5. Khazaeli, M. B., Conry, R. M., and LoBuglio, A. F. Human immune response to monoclonal antibodies. J. Immunother., *15:* 42–52, 1994.

6. Buchsbaum, D. J. Experimental radioimmunotherapy and methods to increase therapeutic efficacy. *In:* D. M. Goldenberg (ed.), Cancer Therapy with Radiolabeled Antibodies, pp. 115–140. Boca Raton, FL: CRC Press, 1995.

7. Thor, A., Ohuchi, N., Szpak, C., Johnston, W., and Schlom, J. The distribution of oncofetal antigen TAG-72 defined by monoclonal antibody B72.3. Cancer Res., *46:* 3118–3124, 1986.

8. LoBuglio, A. F., Wheeler, R. H., Trang, J., Haynes, A. M., Rogers, K., Harvey, E. B., Sun, L., Ghrayeb, J., and Khazaeli, M. B. Mouse/human chimeric monoclonal antibody in man: kinetics and immune response. Proc. Natl. Acad. Sci. USA, *86:* 4220–4224, 1989.

9. Meredith, R. F., LoBuglio, A. F., Plott, W. E., Orr, R. A., Brezovich, I. A., Russell, C. D., Harvey, E. B., Yester, M. V., Wagner, A. J., Spencer, S. A., Wheeler, R. H., Saleh, M. N., Rogers, K. J., Polansky, A., Salter, M. M., and Khazaeli, M. B. Pharmacokinetics, immune response, and biodistribution of iodine-131-labeled chimeric mouse/human IgGI, 17–1A monoclonal antibody. J. Nucl. Med., *32:* 1162–1168, 1991.

10. Slavin-Chiorini, D. C., Kashmiri, S. V. S., Schlom, J., Calvo, B., Shu, L. M., Schott, M. E., Milenic, D. E., Snoy, P., Carrasquillo, J., Anderson, K., and Horan Hand, P. Biological properties of chimeric domain-deleted anticarcinoma immunoglobulins. Cancer Res., *55* (Suppl.): 5957s–5967s, 1995.

11. Raben, D., Buchsbaum, D. J., Khazaeli, M. B., Rosenfeld, M. E., Gillespie, G. Y., Grizzle, W. E., Liu, T., and Curiel, D. T. Enhancement of radiolabeled antibody binding and tumor localization through adenoviral transduction of the human carcinoembryonic antigen gene. Gene Ther., *3:* 567–580, 1996.

12. Buchsbaum, D. J., Raben, D., Stackhouse, M. A., Khazaeli, M. B., Rogers, B. E., Rosenfeld, M. E., Liu, T., and Curiel, D. T. Approaches to enhance cancer radiotherapy employing gene transfer methods. Gene Ther., *3:* 1042–1068, 1996.

13. Rosenfeld, M. E., Rogers, B. E., Khazaeli, M. B., Mikheeva, G., Raben, D., Mayo, M. S., Curiel, D. T., and Buchsbaum, D. J. Adenoviral mediated delivery of gastrin releasing peptide receptor results in specific tumor localization of a bombesin analogue *in vivo*. Clin. Cancer Res., *3:* 1187–1194, 1997.

14. Rogers, B. E., Curiel, D. T., Mayo, M. S., Laffoon, K., Bright, S., and Buchsbaum, D. J. Tumor localization of a radiolabeled bombesin analogue in mice bearing human ovarian tumors induced to express the gastrin releasing peptide receptor by an adenoviral vector. Cancer (Phila.), *80:* 2419–2424, 1997.

15. Rogers, B. E., Rosenfeld, M. E., Khazaeli, M. B., Mikheeva, G., Stackhouse, M. A., Liu, T., Curiel, D. T., and Buchsbaum, D. J. Localization of iodine-125-mIP-Des-Met^{14}-bombesin (7–13)NH$_2$ in

ovarian carcinoma induced to express the gastrin releasing peptide receptor by adenoviral vector-mediated gene transfer. J. Nucl. Med., *38:* 1221–1229, 1997.

16. Rogers, B. E., McLean, S. F., Kirkman, R. L., Della Manna, D., Bright, S. J., Olsen, C. C., Myracle, A. D., Mayo, M. S., Curiel, D. T., and Buchsbaum, D. J. *In vivo* localization of [^{111}In]-DTPA-D-Phe^{1}-octreotide to human ovarian tumor xenografts induced to express the somatostatin receptor subtype 2 using an adenoviral vector. Clin. Cancer Res., *3:* 383–393, 1999.

17. Rogers, B. E., Anderson, C. J., Mayo, M. S., Bright, S. J., Olsen, C. C., Lanahan, M. V., Kirkman, R. L., Curiel, D. T., and Buchsbaum, D. J. Localization of Cu-64-TETA-octreotide to human ovarian cancer xenografts induced to express SSTr2 with an adenoviral vector. J. Nucl. Med., *39:* 63P, 1998.

18. Woltering, E. A., O'Dorisio, M. S., and O'Dorisio, T. M. The role of radiolabeled somatostatin analogs in the management of cancer patients. *In:* V. T. DeVita, Jr., S. Hellman, and S. A. Rosenberg (eds.), Principles and Practice of Oncology, PPO Updates, pp. 1–16. Philadelphia: Lippincott-Raven, 1995.

19. Smith-Jones, P. M., Stolz, B., Albert, R., Ruser, G., Macke, H., Briner, U., Tolesvai, L., Weckbecker, G., and Bruns, C. Synthesis, radiolabelling, and evaluation of DTPA/octreotide conjugates for radiotherapy. J. Labelled Compd. Radiopharm., *37:* 499–501, 1995.

20. Anderson, C. J., Jones, L. A., Bass, L. A., Sherman, E. L. C., McCarthy, D. W., Cutler, P. D., Lanahan, M. V., Cristel, M. E., Lewis, J. S., and Schwarz, S. W. Radiotherapy, toxicity and dosimetry of copper-64-TETA-octreotide in tumor-bearing rats. J. Nucl. Med., *39:* 1944–1951, 1998.

21. Zamora, P. O., Gulhke, S., Bender, H., Diekmann, D., Rhodes, B. A., Hans-Jurgen, B., and Knapp, F. F., Jr. Experimental radiotherapy of receptor-positive human prostate adenocarcinoma with ^{188}Re-RC-160, a directly-radiolabeled somatostatin analogue. Int. J. Cancer, *65:* 1–8, 1996.

22. Stolz, B., Weckbecker, G., Smith-Jones, P. M., Albert, R., Raulf, F., and Bruns, C. The somatostatin receptor-targeted radiotherapeutic [^{90}Y-DOTA-DPhe^{1}, Tyr^{3}]octreotide (^{90}Y-SMT 487) eradicates experimental rat pancreatic CA 20948 tumours. Eur. J. Nucl. Med., *25:* 668–674, 1998.

23. Kashmiri, S. V. S., Shu, L., Padlan, E. A., Milenic, D. E., Schlom, J., and Horan Hand, P. Generation, characterization, and *in vivo* studies of humanized anticarcinoma antibody CC49. Hybridoma, *14:* 461–473, 1995.

24. Slavin-Chiorini, D. C., Kashmiri, S. V. S., Lee, H-S., Milenic, D. E., Poole, D. J., Bernon, E., Schlom, J., and Horan Hand, P. A CDR-grafted (humanized) domain-deleted antitumor antibody. Cancer Biother. Radiopharm., *12:* 305–316, 1997.

25. Fraker, P. J., and Speck, J. C. Protein and cell membrane iodinations with a sparingly soluble chloroamide, 1, 3, 4, 6-tetrachloro-3α, 6α-diphenylglycoluril. Biochem. Biophys. Res. Commun., *80:* 849–857, 1978.

26. Chappell, L. L., Rogers, B. E., Khazaeli, M. B., Mayo, M. S., Buchsbaum, D. J., and Brechbiel, M. W. Improved synthesis of the bifunctional chelating agent 1, 4, 7, 10-tetraaza-*N*-(1-carboxy-3-(4 nitrophenyl)propyl)-*N′*, *N″*, N‴-tris(acetic acid) cyclododecane (PA-DOTA). Bioorg. & Med. Chem. Lett., in press, 1999.

27. Anderson, C. J., Pajeau, T. S., Edwards, W. B., Sherman, E. L. C., Rogers, B. E., and Welch, M. J. *In vitro* and *in vivo* evaluation of copper-64-octreotide conjugates. J. Nucl. Med., *36:* 2315–2325, 1995.

28. Wickham, T. J., Carrion, M. E., and Kovesdi, I. Targeting of adenovirus penton base to new receptors through replacement of its RGD motif with other receptor-specific peptide motifs. Gene Ther., *2:* 750–756, 1995.

29. Wickham, T. J., Segal, D. M., Roelvink, P. W., Carrion, M. E., Lizonova, A., Lee, G. M., and Kovesdi, I. Targeted adenovirus gene transfer to endothelial and smooth muscle cells by using bispecific antibodies. J. Virol., *70:* 6831–6838, 1996.

30. Wickham, T. J., Roelvink, P. W., Brough, D. W., and Kovesdi, I. Adenovirus targeted to heparan-containing receptors increases its gene delivery efficiency to multiple cell types. Nat. Biotechnol., *14:* 1570–1573, 1996.

31. Douglas, J. T., Rogers, B. E., Rosenfeld, M. E., Michael, S. I., Feng, M., and Curiel, D. T. Targeted gene delivery by tropism-modified adenoviral vectors. Nat. Biotechnol., *14:* 1574–1578, 1996.

32. Goldman, C. K., Rogers, B. E., Douglas, J. T., Sosnowski, B. A., Ying, W., Siegal, G. P., Baird, A., Campain, J. A., and Curiel, D. T. Targeted gene delivery to Kaposi's sarcoma cells via the fibroblast growth factor receptor. Cancer Res., *57:* 1447–1451, 1997.

33. Wickham, T. J., Tzeng, E., Shears, L. L. n., Roelvink, P. W., Li, Y., Lee, G. M., Brough, D. E., Lizonova, A., and Kovesdi, I. Increased *in vitro* and *in vivo* gene transfer by adenovirus vectors containing chimeric fiber proteins. J. Virol., *71:* 8221–8229, 1997.

34. Rogers, B. E., Douglas, J. T., Sosnowski, B. A., Ying, W., Pierce, G., Buchsbaum, D. J., Della Manna, D., Baird, A., and Curiel, D. T. Enhanced *in vivo* gene delivery to human ovarian cancer xenografts utilizing a tropism-modified adenovirus vector. Tumor Targeting, *3:* 25–31, 1998.

35. Watkins, S. J., Mesyanzhinov, V. V., Kurochkina, L. P., and Hawkins, R. E. The 'adenobody' approach to viral targeting: specific and enhanced adenoviral gene delivery. Gene Ther., *4:* 1004–1012, 1997.

36. Wickham, T. J., Lee, G. M., Titus, J. A., Sconocchia, G., Bakacs, T., Kovesdi, I., and Segal, D. M. Targeted adenovirus-mediated gene delivery to T cells via CD3. J. Virol., *71:* 7663–7669, 1997.

37. Stackhouse, M. A., Buchsbaum, D. J., Kancharla, S. R., Grizzle, W. E., Grimes, C., Laffoon, K., Pederson, L. C., and Curiel, D. T. Specific membrane receptor gene expression targeted with radiolabeled peptide employing the erbB-2 and DF3 promoter elements in adenoviral vectors. Cancer Gene Ther., *6:* 209–219, 1999.

Clinical Cancer Research

Targeting Strategies for Cancer Radiotherapy

Donald J. Buchsbaum, Buck E. Rogers, M. B. Khazaeli, et al.

Clin Cancer Res 1999;5:3048s-3055s.